

Journal of Biomedical Optics

SPIEDigitalLibrary.org/jbo

Microstructured optical fiber interferometric breathing sensor

Fernando C. Favero
Joel Villatoro
Valerio Pruneri



SPIE

Microstructured optical fiber interferometric breathing sensor

Fernando C. Favero,^{a,b} Joel Villatoro,^b and Valerio Pruneri^{b,c}

^aPontifical Catholic University of Rio de Janeiro, Rua Marquês de São Vicente 225, 22453-900, Rio de Janeiro, Brazil

^bICFO-The Institute of Photonic Sciences, Mediterranean Technology Park, Av. Carl Friedrich Gauss, number 3, 08860 Castelldefels, Barcelona, Spain

^cICREA-Institució Catalana de Recerca i Estudis Avançats, 08010, Barcelona, Spain

Abstract. In this paper a simple photonic crystal fiber (PCF) interferometric breathing sensor is introduced. The interferometer consists of a section of PCF fusion spliced at the distal end of a standard telecommunications optical fiber. Two collapsed regions in the PCF caused by the splicing process allow the excitation and recombination of a core and a cladding PCF mode. As a result, the reflection spectrum of the device exhibits a sinusoidal interference pattern that instantly shifts when water molecules, present in exhaled air, are adsorbed on or desorbed from the PCF surface. The device can be used to monitor a person's breathing whatever the respiration rate. The device here proposed could be particularly important in applications where electronic sensors fail or are not recommended. It may also be useful in the evaluation of a person's health and even in the diagnosis and study of the progression of serious illnesses such as sleep apnea syndrome. © 2012 Society of Photo-Optical Instrumentation Engineers (SPIE). [DOI: 10.1117/1.JBO.17.3.037006]

Keywords: fiber optic sensors; interferometers; interferometry; optical breathing sensors.

Paper 11503 received Sep. 13, 2011; revised manuscript received Jan. 5, 2012; accepted for publication Jan. 13, 2012; published online Mar. 23, 2012.

1 Introduction

Breathing is a human vital sign, thus its monitoring is important during certain imaging and surgical procedures where the patient needs to be sedated or anesthetized.¹ On the other hand, some serious illnesses (e. g. sleep apnea syndrome) can be diagnosed by detecting alterations in breathing rates or abnormal respiratory rate.² Monitoring of breathing is also important to study the progression of a diagnosed illness or to evaluate the health of a person.

Breathing can be detected and analyzed using different methods. The most popular ones involve electronic sensors, see for example Refs. 3 and 4. Electronic breathing sensors are not recommended when patients are, for example, in a magnetic resonance imaging (MRI) system, or during any oncological treatment that requires the administration of radiation or high electric/magnetic fields since they can fail and also represent a burning hazard to the patient. In the aforementioned conditions optical breathing sensors are good candidates. Breathing can be monitored, for example, using fiber-based humidity or temperature sensors placed close to the patient's nose or mouth since the air exhaled by these airways has higher humidity and is warmer than the inhaled air.⁵⁻⁹ Another alternative to monitor breathing using optical fiber sensors is by detecting the contraction and expansion of the patient's chest and abdomen that occur during breathing.¹⁰⁻¹⁴ This can be done by means of highly-sensitive strain, bending or pressure sensors set in a belt, strap or patch attached to the patient's body.¹⁰⁻¹⁴

The advantages of fiberoptic sensors for monitoring breathing and other parameters of clinical relevance include their small size, bio- and electromagnetic compatibility and greater

flexibility. Some drawbacks of the existing fiber-based breathing sensors include the need of temperature/humidity-sensitive thin films which usually degrade over time or respond too slowly to changes in humidity/temperature. On the other hand, some fiber-based strain/bending sensors are also sensitive to body motions, thus, in some circumstances; it can be difficult to distinguish breathing from a person's involuntary motions.

In this work we report on a simple optical fiber interferometric breathing sensor that does not require any kind of breathing-sensitive thin film or layer. The device operates in reflection mode and consists of a short segment of photonic crystal fiber (PCF), also known as microstructured or holey optical fiber, fusion spliced at the distal end of a standard optical fiber. A core and a cladding mode are excited and recombined in the PCF. As a result, the reflection spectrum of the device exhibits a well-defined interference pattern. The cladding mode is highly sensitive to water molecules adsorbed on the PCF surface. Thus, when a person exhales air close to the interferometer an instant shift of the interference pattern is observed. The device here proposed may be used to monitor a person's breathing whatever the respiration rate.

2 Device Fabrication and Performance

Figure 1 shows schematic drawings of the proposed device along with some details of the interrogation set up. The fabrication of the interferometer is simple and straightforward since it only involves cleaving and fusion splicing, which can be carried out with common fiber tools and equipment.¹⁵ A micrograph of the PCF cross section is shown in the figure. The fiber is commercially available and it is known as large-mode-area PCF (LMA-10, NKT Photonics). This fiber has six-fold symmetry; its core and outer diameters are, respectively, 10 and

Address all correspondence to: Joel Villatoro, ICFO—The Institute of Photonic Sciences, Mediterranean Technology Park, Av. Carl Friedrich Gauss, num. 3, 08860 Castelldefels, Barcelona, Spain, Tel: 34935534137; Fax: 34 935534000; E-mail: joel.villatoro@icfo.es

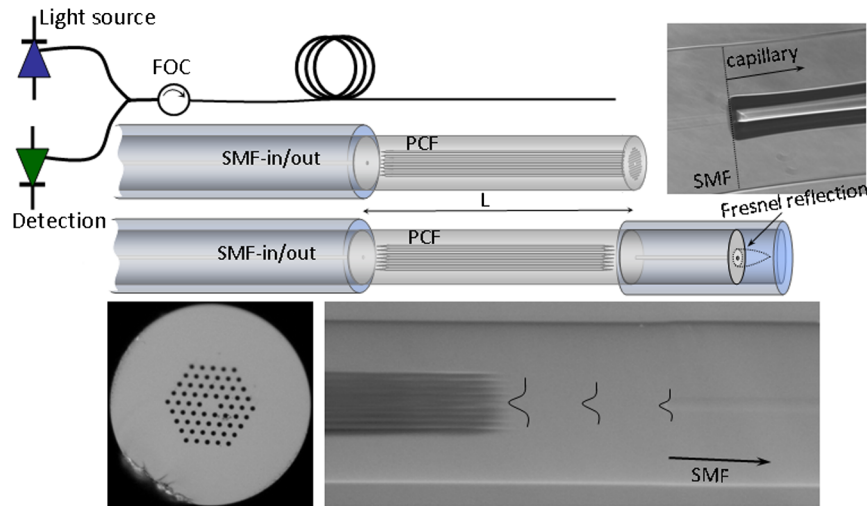


Fig. 1 Schematic diagram for interrogating the interferometer. The drawings show the interferometer with an “open void” or a “sealed void” configuration. L is the length of PCF. The micrographs show the PCF cross section and the PCF-SMF or SMF-capillary junctions. The broadening of the fundamental SMF mode is also illustrated.

125 μm . The diameter of the voids is 3.1 μm and the separation between consecutive voids (pitch) is 6.6 μm . A short section (between 1 to 2 cm) of PCF was fusion spliced at the end of a standard telecommunication optical fiber (SMF-28). A conventional splicing machine (Ericsson FSU 955) was used to fabricate the devices. The default programs set in such a machine for splicing single mode fibers can be used to splice the SMF and the PCF. Under these conditions a robust and permanent joint is achieved. However, the PCF’s voids fully collapse over a length of a few hundred micrometers because the softening point of PCFs is lower than that of SMFs due to their holey structure. The length of the collapsed zone in the PCF can be shortened without compromising the robustness of the splice by properly reducing the intensity and duration of the arc discharge.¹⁶ Figure 1 shows a micrograph of the SMF-PCF junction with a 130 μm -long collapsed zone.

The collapsed region in the PCF is what allows the excitation and recombination of modes, thus achieving an interferometer. The propagating beam goes through a section without core or voids when it travels through the SMF-PCF junction. When the fundamental SMF-in mode enters the collapsed region of the PCF, it immediately broadens due to diffraction, as seen in Fig. 1. The broadening introduces a mode field mismatch which combined with the modal properties of the PCF allows the excitation of specific modes in the PCF.¹⁶ Owing to the axial symmetry the excited modes are those that have similar azimuthal symmetry, i.e., the HE_{11} core mode and the HE_{22} -like cladding mode.¹⁶ Such modes have different effective refractive indices and propagate at different phase velocities; hence they accumulate a phase difference. If the effective index of the HE_{11} core mode is n_1 and n_2 is that of the HE_{22} cladding mode, then the phase difference will be $\Delta\phi \cong 2\pi\Delta n/L$, with $\Delta n = n_1 - n_2$ and L the length of PCF. The effective indices, and therefore, the phase difference $\Delta\phi$ depend on the wavelength (λ) of the optical source. If the modes are reflected from the PCF cleaved end, as seen in the “open void” configuration in Fig. 1, the accumulated phase difference will be $\Delta\phi \cong 4\pi\Delta n/L$ due to the double pass over the PCF.^{17,18} When the reflected modes reach the collapsed region they will

be recombined into a SMF core mode. Thus, if one launches light from a broadband optical source, e.g. an light emitting diode (LED), to the device and the output light is fed to a spectrometer; the resulting spectrum will exhibit a series of maxima and minima, i.e. an interference pattern as it is shown in Fig. 2(a).

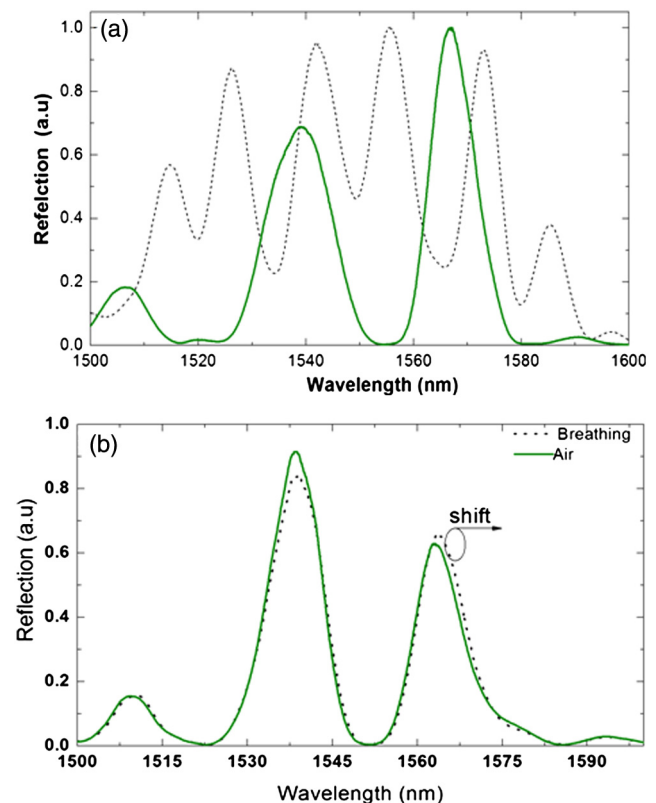


Fig. 2 (a) Normalized reflection spectra of an interferometer with in an open void configuration (dotted line) and in a sealed void one (solid line). (b) Reflection spectrum of a sealed-void interferometer when the external medium was air (solid line) and when a person breathed close to it (dotted line). In all cases the length of PCF was 20 mm.

The open voids at the end of the PCF allow the sensing of chemical vapor or humidity^{17,18} but with slow response time. In addition, it is not easy to clean the voids of the PCF when they are infiltrated with moisture or dust particles. Thus, a “sealed void” configuration was devised, see Fig. 1. The sealing of the PCF voids was carried out by splicing ~10 mm of SMF to the PCF, by collapsing also the PCF holes, and by splicing ~5 mm of a capillary tube with inner/outer diameters of 40/125 μm to the SMF. The end of the capillary tube was sealed by means of arc discharges in the splicing machine. Note that the capillary tube at the end of the SMF completely isolates and protects the glass-air interface that functions as a low-reflectivity mirror (Fresnel reflection). The reflection spectrum of a 2-cm-long interferometer with sealed PCF voids is shown in Fig. 2(b). Although both interferometers were fabricated with the same length of PCF they exhibit different periods and visibility. This is probably due to the fact that the cladding mode propagates with high losses. In the interferometer with the sealed void configuration the cladding mode does experience Fresnel reflection as the core mode. In fact, the cladding mode can be completely absorbed by the protective coating of the SMF located at the distal end. Therefore, in such an interferometer the fundamental mode reflected from the short section of SMF is what excites a core and a cladding mode in the PCF. The visibility of the interference pattern increases remarkably since the cladding mode propagates only once over the PCF. Thus, in the sealed void interferometer the accumulated phase difference depends only on the physical length of PCF in spite of the fact that the device operates in reflection mode.

When a guided mode reaches the waveguide-external-medium interface it becomes highly sensitive to refractive index changes that occur right at the waveguide’s surface. Such properties can be exploited for direct optical sensing, i.e., no intermediate layer, material or periodic structure is needed.^{17–20} In our interferometer with the sealed void configuration, absorption of water vapor (humidity) or a nanometer-thick polymeric or dielectric layer on the PCF surface will modify solely the phase velocity (or effective refractive index) of the cladding mode, because the core mode is completely isolated from the external medium. As a consequence, the phase difference between the interfering modes will change and the interference pattern will shift. Figure 2 shows the reflection spectra of an interferometer in the sealed void configuration when the external medium was air and when a person exhaled

air directly on the PCF. It can be noted that the peaks of the interference pattern experience a minute but detectable shift to longer wavelengths. Thus, by tracking the position of the peaks of the interference pattern of our interferometer a person’s breathing can be monitored.

3 Device Packaging for Monitoring Breathing

Based on the above analysis and observations we proceeded to study the performance of our sealed-void interferometer as a breathing sensor. To do so the interferometer was properly packaged. The fiber that was bare, except the section of PCF, was protected with a glass tube with inner/outer diameters of 150/400 μm which in turn was shielded with another metallic tube with inner/outer diameters of 1.7/3.0 mm. The tube was filled with glue to secure the device. The remaining optical fiber was cabled and a conventional connector was put at the end. Prior to packaging, the thick tube was modified to leave a narrow aperture over the PCF region, thus allowing a person’s exhaled air to enter/exit the sensitive part of the interferometer, as seen in Fig. 3. The packaged device was then set in an inexpensive, disposable silicone oxygen mask which in turn was attached to a volunteer’s nose and mouth and secured with the elasticized headband of the mask. The sensor was set in such a way that it was approximately at 3 cm from the patient’s nose. It is important to point out that we ensured that the light from the end of the interferometer never reached the volunteer’s eyes, face or skin even though the power of our optical source was in the microwatt level. The shift of the interference pattern was monitored with a commercial fiber Bragg grating (FBG) interrogator (I-MON E-USB, Ibsen Photonics). One point was collected every 16 ms. Such a sampling rate is fast enough to monitor the breathing of any person. Figure 3 shows the shift of the interference pattern as a function of time when a person was breathing normally. The measurements were carried out with the set-up shown schematically in Fig. 1; the light source was an LED with central emission at 1550 nm. The volunteer heart rate was 85 beats per minute (bpm), the same that was measured with a commercial heart rate monitor attached with a strap to the volunteer’s chest.

To investigate further the capability of our device, we monitored our volunteer’s breathing at different conditions. The volunteer was subjected during a few minutes to an intense aerobic exercise until his heart rate reached 110 or 135 bpm. Immediately after the exercise, the mask with the referred sensor

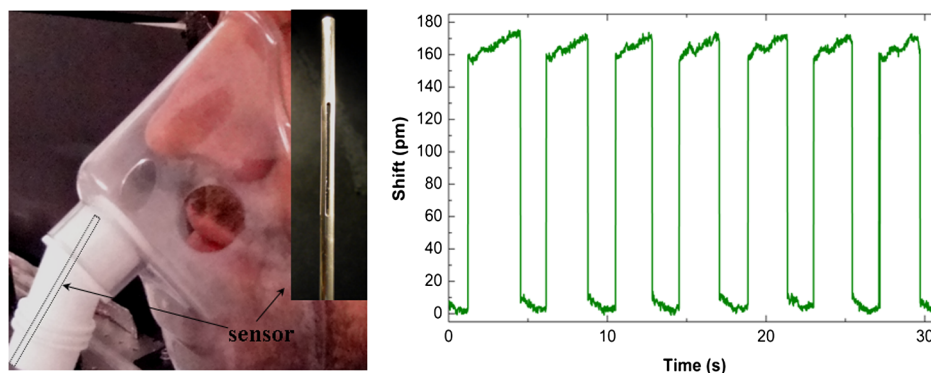


Fig. 3 Photograph of the mask placed on the volunteer’s face showing the position of the sensor inside the mask (dotted rectangle). The exhaled air stems the interior of the mask and the PCF surface. The inset picture shows the tip of the packaged sensor wherein with the aperture is located. The plot shows the shift of the interference pattern when a person was breathing normally. A 20-mm-long sealed-void interferometer was used. The light source was an LED with central emission at 1550 nm and the measurements were carried out with a set-up similar to that illustrated in Fig. 1.

was placed over his nose and mouth and his breathing was again monitored. Figure 4 shows the observed shift versus time. It can be noted that the device responds well whatever the respiration cycle. In another test, the volunteer was asked to breathe normally and then to stop breathing during a few seconds. Figure 5(a) shows the results under these breathing conditions. It can be noted that the shift is nearly zero during the entire time the volunteer did not breathe. The results shown in Fig. 5(a) suggest that our device might be useful in the study or diagnosis of sleep apnea syndrome, an illness characterized by abnormal pauses in breathing or instances of abnormally low breathing during sleep.

To investigate the reusability of our sensor, the breathing of another volunteer was monitored; the results are shown in Fig. 5(b). The monitoring was carried out with the same procedure described above. Note that the shift is not exactly the same in all cases due to variation in the separation between the person's nose and the sensor, and also to possible contamination of the sensitive part of the interferometer. However, information about the person's respiration rate, an important indicator of a person's health, is obtained. The contamination issue can be overcome by cleaning the sensor with commercially available solvents or even with sterilization of the device since optical fibers can be sterilized but fluctuations of the separation between nose and sensor cannot be eliminated.

The results discussed above are promising, because they indicate that our device can follow the breathing cycles whatever the respiration rate or condition. However, for the device to be useful as a patient respiratory sensor in a real medical setting it would need to fulfill more requirements. For example, the limitations in size were analyzed by fabricating interferometers of

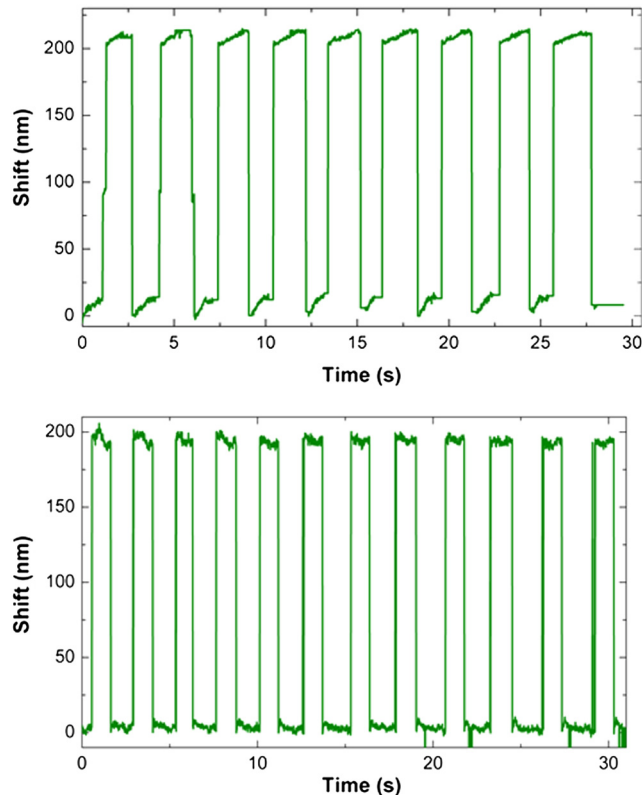


Fig. 4 Shift of the interference pattern observed when the volunteer's heart beat rate was 110 bpm (top graph) and 135 bpm (bottom graph). In both cases a 20-mm-long sealed-void interferometer was used and the wavelength was 1550 ± 50 nm.

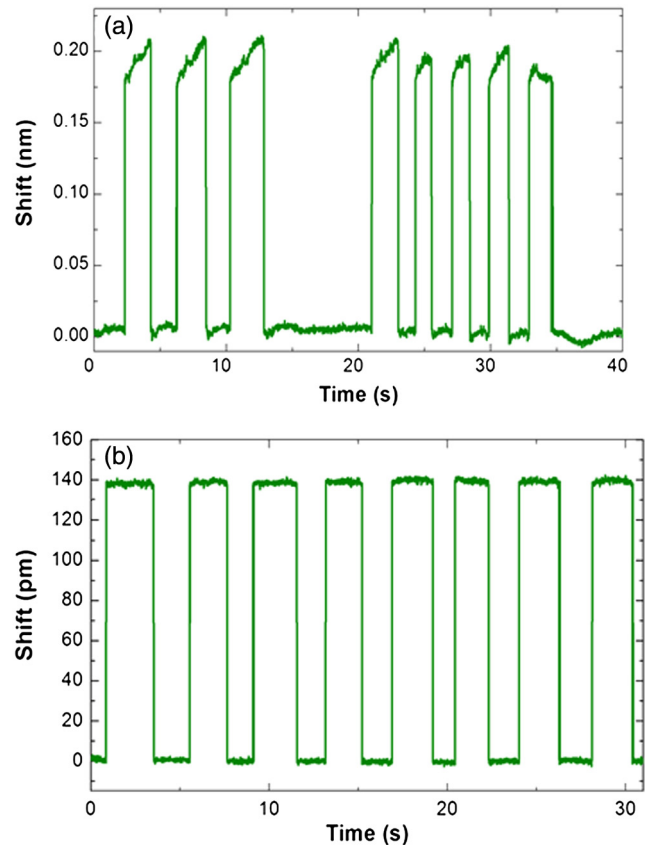


Fig. 5 (a) Shift of the interference pattern when a person, on purposefully, stopped breathing during a few seconds. (b) Shift of the interference pattern observed when another volunteer was breathing normally. In both cases a 20-mm-long sealed-void interferometer was used and the wavelength was 1550 nm.

different lengths. Possible failure modes were also investigated. Figure 6 shows the interference pattern observed in a 12-mm-long device when the fiber cable was subjected to movements and bending which typically can be caused by motion of the patient. Although the intensity of the pattern fluctuates the position of the peak remains unaltered. This suggests that voluntary

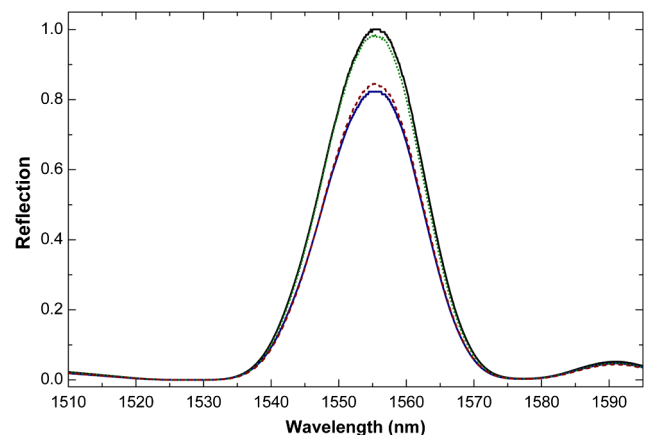


Fig. 6 Interference patterns observed when the fiber was subjected to bending and movements. Each trace is the result from a different position. The length of PCF was 12 mm. The intensity changes but the position of the peak remains unaltered.

or involuntary motions of the patient or fiber cable may not affect the measurements. Another possible failure mode is when a person coughs or contaminates the device with fluids (saliva, sputum, etc.). However, these issues can be avoided or overcome by embedding the device in a nasal clip, adequate packaging, or using a cleaning process.

4 Conclusions

In this work we report on a breathing sensor based on a photonic crystal fiber interferometer that operates in reflection mode. The fabrication of the device is simple since it involves a pair of fusion splices, hence it can be carried out with conventional fiber tools and instruments. The cost of the devices is low because the components (optical fibers) are inexpensive and widely available. The key part of the interferometer is a microscopic collapsed region in the PCF which is what allows the excitation and recombination of two modes in the PCF. One of the modes (the cladding mode) is highly sensitive to changes of refractive index on the PCF surface. Thus, when water vapor from exhaled air is present on the PCF surface, the interference pattern shifts. Such a shift can be detected in real time. Our results suggest that the device can be used to monitor a person's breathing whatever the breathing rate is. All the components of the interferometer are (or can be made of) dielectric materials, thus, the device can be used in critical applications, such as during magnetic resonance imaging or some oncological treatments, where electrical breathing sensors may not operate properly or are not recommended because of potential burning hazards. The device here proposed can also be useful in the diagnosis of serious illnesses such as sleep apnea syndrome.

Development of a portable breathing monitor is feasible because of considerable advances in the development of miniature light sources and detectors. Compact and portable FBG interrogator units are emerging. Thus, in the near future the breathing sensors here proposed might be incorporated into battery-operated portable medical diagnostic equipment.

Acknowledgments

This work was supported by the Ministerio de Ciencia e Innovación (Spain) under project TEC2010-14832, the Brazilian Coordenação de Aperfeiçoamento Pessoal de Nível Superior (251710-8 PhD Fellowship) and the Fundació Privada Cellex Barcelona. The authors are grateful to Walter Margulis from ACREO, Sweden, for the capillaries used in this work.

References

1. M. Folke et al., "Critical review of non-invasive respiratory monitoring in medical care," *Med. Biol. Eng. Comput.* **41**(4), 377-383 (2003).
2. P. Várady et al., "A novel method for the detection of apnea and hypopnea events in respiration signals," *IEEE Trans. Biomed. Eng.* **49**(9), 936-942 (2002).
3. P. Corbishley and E. Rodríguez-Villegas, "Breathing detection: towards a miniaturized, wearable, battery-operated monitoring system," *IEEE Trans. Biomed. Eng.* **55**(1), 196-204 (2008).
4. F. Q. AL-Khalidi et al., "Respiration rate monitoring methods: a review," *Pediatr. Pulm.* **46**(6), 523-529 (2011).
5. S. Muto, H. Sato, and T. Hosaka, "Optical humidity sensor using fluorescent plastic fiber and its application to breathing-condition monitor," *Jpn. J. Appl. Phys.* **33**(10), 6060-6064 (1994).
6. F. J. Arreguil et al., "Optical fiber humidity sensor using a nano Fabry-Perot cavity formed by the ionic self-assembly method," *Sensor Actuat B -Chem.* **59**(1), 54-59 (1999).
7. Y. Kang et al., "Nanostructured optical fibre sensors for breathing airflow monitoring," *Meas. Sci. Technol.* **17**(5), 1207-1212 (2006).
8. W. J. Yoo et al., "Development of optical fiber-based respiration sensor for noninvasive respiratory monitoring," *Opt. Rev.* **18**(1), 132-138 (2011).
9. S. Akita, A. Seki, and K. Watanabe, "A monitoring of breathing using a hetero-core optical fiber sensor," *Proc. SPIE* **7981**, 79812W (2011).
10. A. Babchenko et al., "Fiber optic sensor for the measurement of respiratory chest circumference changes," *J. Biomed. Opt.* **4**(2), 224-229 (1999).
11. G. Wehrle et al., "A fiber optic Bragg grating strain sensor for monitoring ventilatory movements," *Meas. Sci. Technol.* **12**(7), 805-809 (2001).
12. A. Grillet et al., "Optical fiber sensors embedded into medical textiles for healthcare monitoring," *IEEE Sens. J.* **8**(7), 1215-1222 (2008).
13. M. Nishiyama, M. Miyamoto, and K. Watanabe, "Respiration and body movement analysis during sleep in bed using hetero-core fiber optic pressure sensors without constraint to human activity," *J. Biomed. Opt.* **16**(1), 017002 (2011).
14. A. F. Silva et al., "Simultaneous cardiac and respiratory frequency measurement based on a single fiber Bragg grating sensor," *Meas. Sci. Technol.* **22**(7), 075801 (2011).
15. J. Villatoro et al., "Simple all-microstructured-optical-fiber interferometer built via fusion splicing," *Opt. Express* **15**(4), 1491-1496 (2007).
16. G. A. Cárdenas-Sevilla et al., "Photonic crystal fiber sensor array based on modes overlapping," *Opt. Express* **19**(8), 7596-7602 (2011).
17. J. Villatoro et al., "Photonic crystal fiber interferometer for chemical vapor detection with high sensitivity," *Opt. Express* **17**(3), 1447-1453 (2009).
18. J. Mathew et al., "Humidity sensor based on photonic crystal fibre interferometer," *Electron. Lett.* **46**(19), 1341-1343 (2010).
19. K. Tiefenthalera and W. Lukosz, "Grating couplers as integrated optical humidity and gas sensors," *Thin Solid Films* **126**(3-4), 205-211 (1985).
20. D. Monzón-Hernández et al., "Photonic crystal fiber microtaper supporting two selective higher-order modes with high sensitivity to gas molecules," *Appl. Phys. Lett.* **93**(8), 081106 (2008).